
Article:
Korus, A., Szlęk, A. and Samson, A. orcid.org/0000-0002-1979-9989 (2019) Physicochemical properties of biochars prepared from raw and acetone-extracted pine wood. Fuel Processing Technology, 185. pp. 106-116. ISSN 0378-3820

https://doi.org/10.1016/j.fuproc.2018.12.004

Physicochemical properties of biochars prepared from raw and acetone-extracted pine wood

Agnieszka Korus[a,b,*], Andrzej Szlęk[a], Abby Samson[b]

[a] Institute of Thermal Technology, Silesian University of Technology, Gliwice, Poland

[b] School of Engineering, University of Lincoln, Lincoln, Lincolnshire LN6 7TS, UK

Abstract

Biochars can be used in a wide range of applications, serving as soil additives, sorbents, fuels, catalyst supports or as catalysts themselves. There is however, a vast range of variables influencing the properties of biochars and their performance as catalysts. One of the characteristic features of pine wood is its high extractives content which is known to influence the pyrolysis process, therefore it can also affect the properties of the derived biochar. In this paper, raw and acetone-extracted pine wood was used to prepare steam-activated biochars. The changes in physicochemical properties of the chars upon the feedstock treatment were examined, including the analysis of surface area, porosity, acidic site distribution, metal content and surface characterisation by FTIR and SEM techniques. A toluene pyrolytic conversion experiment was carried out to determine the chars' potential towards tar removal. At the initial stage of the process, toluene removal was higher for extracted than non-extracted

* Corresponding author. E-mail: agnieszka.korus@polsl.pl (Agnieszka Korus)

pine char, and with time-on-stream their performance became similar. It was concluded that the removal of the extractives affected wood pyrolysis, creating char with significantly higher microporosity and increased acidity. Upon steam activation, the microporosity and acidity of both chars was enhanced in general while the difference between the samples diminished, while still improving toluene conversion in the early stages of the process.

Keywords:

biochar; pyrolysis; extractives

Nomenclature:

P – non-activated pine char

PE – non-activated extracted pine char

PA – activated pine char

PAE – activated extracted pine char

PA_40, PA_50, PA_60 – spent PA char after 40, 50 and 60 min run, respectively

PAE_50, PA_60 – spent PAE char after 50 and 60 min run, respectively

1. Introduction

Utilisation of different biochars for tar catalytic reforming has become a subject of extensive research due to their many advantages. The purpose of the heterogeneous tar conversion is not only to clean the syngas, but also to increase its calorific value. Harvesting biochar, a

gasification by-product, as a conversion catalyst, is a cost-effective and convenient method. The gasification process supplies accessible catalyst that can be utilised after deactivation/poisoning by recirculating it to the gasifier. Despite an increasing interest in biochar catalysts [1–6], their properties, and therefore their suitability for tar removal, vary significantly due to the differences in feedstock and preparation conditions. One of the features of woody biomass that significantly diversifies its properties, is the presence of extractives. These can differ greatly depending on the wood species, origin and age [7,8].

Along with the three main polymeric constituents, cellulose, hemicellulose and lignin, softwood contains substantial amounts of extractives. Among these, a few main groups of compounds can be distinguished: carbohydrates, fatty acids, fatty acid esters, phytosterols, resins, as well as some phenols [9]. These groups can be extracted from wood to a different extent, depending on the polarity of the compound and the solvent used for the extraction. The general rule is that less polar solvents are able to extract only resins, phytosterols, fatty acids and fatty acid esters, while more polar organic solvents additionally remove some phenols and carbohydrates as well as some inorganic species [10]. Mészáros et al. [9] reported, that acetone extraction of *Robinia pseudoacacia* removes most of the lipophilic extractives but it also releases some of the carbohydrates and phenolic compounds.

The pine lipophilic fraction of extractives contains mainly resin acids, fatty acid esters and fatty acids. Hemingway et al. [7,11] studied different pine species extractives in the heartwood and sapwood of trees of different ages. The reported fraction within the extractives composed of resin acids varies significantly from 22.4 to 97 wt.% and it generally increases with age. Regardless of age or part of tree, the main representatives of this group, levopimaric and palustric acid, make up to 50 % of the total resin acids. A significant amount of abietic, neoabietic and pimaric acids can be also found. Fatty acid esters content in pine extractives is reported to be significantly higher than free fatty acids amount – 30-50 wt.% and up to 4 wt.%

69 of total extracted compounds, respectively. The main esters found in pine wood by
70 Hemingway et al. [7,11] were methyl stearate and methyl oleate, which amounted to almost
71 90% of total fatty acids methyl esters. Zinkel also reported, that pine extractives contain about
72 10 times more fatty acid esters than fatty acids, although triglycerides were considered the
73 most abundant type of fatty acid esters [12]. There are also some phytosterols, terpenes and
74 phenolic compounds present in different pine species extracts [9,13,14].

75 Many aspects of the presence of extractives in wood have been studied so far, including
76 effects on biomass pyrolysis, pulping industry and wood technology [8,15,16]. Guo et al. [14]
77 concluded that the presence of extractives increases reactivity of raw biomass during pyrolytic
78 conversion, lowering the activation energy of pine and ash wood. At the same time, they
79 reported that pine wood has significantly higher ethanol extractives content and their
80 pyrolysis occurs at a wider temperature range, although with lower reaction rates as compared
81 to the ash extractives. It was also determined that pine extractives pyrolysis releases more
82 low-temperature volatiles (resulting from e.g. sterols) and more volatiles in general. It was
83 also reported, that pine extractives pyrolysis yields higher amounts of inorganic gases, while
84 more methanol and methane are released from ash extractives, due to higher methoxy groups
85 content in hardwood lignin. Ash extractives also contain more phenolic compounds that
86 release pyrolysis gaseous products at high temperatures of 600 – 800 °C. Lower phenolic
87 compound content in pine extractives was assigned to guaiacyl lignin, characteristic to
88 softwoods, being harder to decompose upon extraction [14]. There is also a significant
89 difference in the pyrolysis products of extracted and non-extracted wood samples. The
90 pyrolysis of an extracted pine yields less acids and significantly more CO_2 and water in
91 comparison to the pyrolysis of raw biomass [14]. It is therefore expected, that extractives are
92 favouring formic acid over levoglucosan formation from cellulose decomposition [17].

Another important observation reported in literature is the influence of extractives on solid, liquid and gaseous product distributions during wood pyrolysis. The presence of extractives in wood enhances char formation at the expense of liquid products. Twofold explanation of this phenomena is given – an increased tar residence time in extracted rich material and a catalytic char-favouring effect of inorganic species that might be removed by polar solvents during extraction [8,18,19].

Previous studies proved that extractives, although comprised of volatile species, can influence pyrolysis. Therefore, it can be expected that they can affect the properties of the biochar created in this process. In this work, authors examined the changes in physicochemical properties arising during the pyrolysis and consecutive steam activation of a pine biochar upon the feedstock extraction with acetone. Additionally, toluene, as a representative tar compound, was selected to perform tests on the catalytic performance of obtained biochars in a heterogeneous pyrolytic conversion experiment.

Improvement in pyrolytic biochar microporosity and acidity was observed after feedstock extraction. The differences in examined properties were largely diminished during the char activation process, however, the activated char from extracted pine performed better at the initial stages of the toluene conversion experiment due to increased microporosity and acidity.

2. Experimental

2.1. Material

For the purpose of this work, pine (*Pinus sylvestris*) from the south of Poland (Silesia) was used. Wood composition (wt. % on dry basis) was determined according to PN-EN ISO 16948:2015-07 standard and was presented in Table 1. Fresh pine wood without bark or knots was dried at 60 °C for 48 h to remove most of the moisture prior to milling with a cutting mill

117 (Testchem, Poland, model LMN-100) and sieving to 250 – 1000 μm particles. Due to its
118 hygroscopic nature, feedstock was further dried at 105 °C for 2 h directly before char
119 preparation. Extracted pine was prepared from a dried wood in a FOSS Soxtec Avanti 2055
120 apparatus. Extraction involved 60 min of boiling and 90 min of rinsing of 3 g of sample with
121 70 mL of acetone. Gravimetrically determined extractives content for 42 repetitions was 8.5
122 ±0.3 wt. %. The proximate analysis of dried original and extracted pine was performed in
123 duplicates, gravimetrically, according to PN-EN ISO 18122:2016-01 and PN-EN ISO
124 18123:2016-01 and the results are presented in Table 1. An ANOVA analysis suggests no
125 significant differences between the two samples. For char preparation, a batch of
126 approximately 20 g of wood was inserted into a vertical quartz tube reactor with i.d. of 27 mm
127 and a heating zone of 300 mm and purged with 0.45 SLPM N_2 flow. Feedstock, supported by
128 a quartz wool bed, was pyrolysed by heating up to 800 °C with an average heating rate of
129 approximately 47 °C/min. The final isotherm was kept for 60 min. After this time, steam was
130 introduced into the reactor. The char was held at 800 °C for 80 min in a flow of 84.5/15.5
131 vol.% N_2/H_2O mixture with the same superficial velocity as during the pyrolysis step. The
132 activated char was cooled down in a N_2 stream and stored in a desiccator. Char preparation
133 conditions (e.g. temperature, steam concentration) were selected based on the parameters
134 reported in similar studies [3,4].

135

136 Table 1. Elemental analysis of pine wood, wt.% on dry basis and proximate analysis of raw
137 and extracted pine wood, wt.% on dry basis

	C, wt.%	**H, wt.%**	**N, wt.%**	**S, wt.%**	**O, wt.% (by diff.)**
pine	52.46	6.28	0.12	0.01	40.93

	Fixed carbon, wt.% (by diff.)	**Ash, wt.%**	**Volatile matter, wt.%**

pine	12.41	0.20 (±0.005)	87.39 (±0.54)
extracted pine	13.33	0.20 (±0.005)	86.47 (±0.33)

138

139 **2.2. Toluene catalytic pyrolysis over a char bed**

140 The toluene conversion experiment was carried out in a vertical quartz tube reactor with i.d.
141 of 20 mm and a heating zone length of 300 mm, enclosed in an electrical furnace (Czylok,
142 Poland, model RSD 30x300/80) . The detailed description of the test rig can be found
143 elsewhere [20]. 0.5 g of pine char was inserted into the reactor and purged with 99.999 % N_2,
144 while being heated to 800 °C. After this time, a constant flow of 6.4 µl/min of toluene (Sigma
145 Aldrich, purity ≥99.8 %) was fed into the reactor by a syringe pump (Kwapisz, Poland, model
146 Duet 20/50) equipped with a 500 µl Agilent syringe. Runs were performed for feeding times
147 between 5 and 60 min, providing the char performance and deactivation with time-on-stream.
148 Toluene concentration in N_2 was maintained at 12.3 g/Nm^3 throughout all experiments.
149 Unreacted toluene and liquid reaction by-products were trapped in impinger bottles filled with
150 dichloromethane (Sigma Aldrich, purity ≥99.8 %). First impinger was kept at room
151 temperature, while the second one was immersed in the bath cooled to -25 °C. The
152 temperature gradient was introduced, because the evaporation of the solvent from the first
153 bottle has been claimed to improve the condensation of liquid products in the following bottle
154 [21]. Two bottles were proved to be sufficient to recover 99.5 % of fed toluene during blank
155 runs. The content of the impingers was analysed with an Agilent 6890N GC-FID with 30 m x
156 0.32 mm x 0.25 µm HP-5 column. The method was set as follows: initial temperature was set
157 to 50 °C and was maintained for 5 min. Then, the temperature was raised to 80 °C at a rate of
158 5 °C/min. The heating rate was then increased to 10 °C/min to a final temperature of 200 °C
159 where it was held for 2 min. The inlet and the detector were kept at 250 °C and a 1 µl
160 injection with a split ratio of 10:1 was made with an Agilent 7893 autosampler. External

161 calibration method was used to determine liquid products content. Sigma Aldrich reagents
162 with purity ≥99.5 % were used for the products identification and standard solutions
163 preparation. Analysis of variance (ANOVA) was used to assess the results, as it is a popular
164 and practical method to test for the significant differences between the sets of data and it has
165 been commonly used in similar studies [2,22]. A significance level α=0.05 was specified as a
166 threshold. When the calculated probability value (*p*-value) is lower than α the rejection of the
167 null hypothesis is justified. Two-way ANOVA analysis of toluene conversion for two factors
168 – char type and experiment time was carried out. Therefore, three null hypothesis were tested:
169 1) there is no significant difference in toluene conversion between the studied chars, 2) there
170 is no significant difference in toluene conversion for different experiment times, 3) the
171 interaction effect between char types and experiment times does not exist. Based on the
172 obtained *p*-values, the first and second null hypothesis were rejected, while the third one
173 proved to be true, i.e. the two studied factors are independent. All experimental runs were
174 carried out in duplicate and the pooled standard deviation for the obtained conversions was
175 0.048.

176 **2.3. Char, wood and extractives characterisation**

177 IR spectra of all samples were obtained by Fourier-transform infrared spectroscopy (FTIR),
178 using a Perkin Elmer Spectrum 100 spectrometer with universal attenuated total reflectance
179 (UATR) accessory equipped with a germanium crystal. Each spectrum had the resolution of 4
180 cm^{-1} and 32 scans per measurement were taken. For each sample, an average of 5
181 measurements is reported in this work. To provide better contact between the sample and the
182 crystal, all solid samples were milled to a fine powder prior to the analysis. For pine
183 extractives, a thin film was used for the measurements.

184 To obtain the acidic sites distribution, Boehm titrations were performed according to a
185 method standardised by Goertzen et al. [23,24]. Char samples (1 g) were shaken for 24 h with
186 0.05 M solution of either NaOH, Na_2CO_3 or $NaHCO_3$, and then filtrated on Grade 1 Whatman
187 filter papers. A 10 mL aliquot portion was mixed with 10 mL (20 mL for Na_2CO_3) of 0.05 M
188 HCl, purged with N_2 flow of ca. 0.25 mL/min for 2 h and back-titrated with 0.05 M NaOH
189 with N_2 purging. The Boehm method was originally designed for carbon blacks. Since
190 biomass chars contain significant amounts of mobile species, such as metal cations or labile
191 organic carbon (e.g. humic acids [25]), it is advised to wash biochars prior to the acidic sites
192 analysis. Therefore, following the procedure established by Tsechansky and Graber [26], all
193 samples were shaken for 24 h in HCl, followed by 24-h of washing with NaOH to remove all
194 mobile species. Finally, chars were shaken with HCl for another 24 h to protonate all acidic
195 sites. Chars were thoroughly washed with distilled water after each shaking step and then
196 dried at 40 °C prior to the treatment with Boehm bases.

197 Alkali and alkaline earth metals (AAEM) content in the chars was determined by a SpectrAA
198 880 Varian Atomic Absorption Spectrometer after digestion with HNO_3 in a Milestone
199 MLS1200 MEGA microwave. Surface area and porosity measurements were outsourced to
200 the Centre for Functional Nanometrics at Maria Skłodowska Curie University. Samples were
201 outgassed at 100 °C prior to the analysis with a Micromeritics ASAP 2420 instrument by N_2
202 adsorption at -196 °C. Surface area was determined from BET model, micropore area and
203 volume was calculated by t-Plot method. Meso- and macropore volume was obtained from
204 BJH adsorption isotherm. Scanning electron micrographs were taken with a JCM-5000
205 NeoScope microscope.

206 Pine wood and its extractives pyrolysis was studied with a Netzsch STA 409 LUXX
207 thermogravimetric analyser (TGA). 5 mg of the sample was heated up in 100 mL/min N_2 flow
208 up to 800 °C with a heating rate of either 10 or 50 °C/min. Thermogravimetric derivative

209 (DTG) curve of the mass loss function was used to determine the changes in wood pyrolytic
210 conversion in the presence/absence of extractives. DTG curves were further deconvoluted into
211 a set of Gaussian functions to provide an insight into conversion of individual wood
212 compounds. Thermogravimetric analysis was also performed to determine the reactivity of
213 chars during oxidation. Measurements were performed with a Netzsch TG 209 F3 Tarsus
214 instrument in a 12/88 vol.% O_2/N_2 mixture with a total flow of 85 mL/min and a heating rate
215 of 10 °C/min. Char particles were milled and sieved under 36 μm to diminish mass and heat
216 transfer limitations. Kinetic parameters were calculated by temperature integral
217 approximation method using Senum and Yang's 4th degree rational approximation [27].

218 **3. Results and discussion**

219 **3.1. FTIR of pine wood and its extractives**

220 The wood difference FTIR spectrum, i.e. a spectrum obtained by the subtraction of the
221 extracted pine spectrum from the non-extracted pine one, is presented in Fig. 1. It is compared
222 with the spectrum obtained for a thin film of extractives.

223 Despite general similarity between both spectra, some differences can be distinguished. The
224 intensity of the bands in a fingerprint area is relatively high in extractives spectrum, while it is
225 less pronounced in the difference spectrum. Bands in the extractive spectrum are also
226 generally sharper, since they correspond to a relatively limited variety of extracted
227 compounds, while the changes in the wood structure registered by the difference spectrum
228 include the loss of extracted compounds as well as some possible changes to the wood
229 polymeric structure. Those changes might result from simple mechanical removal of acetone-
230 soluble compounds but also some alterations in the structure of polymers are feasible. The
231 release of some simple sugars from hemicellulose or phenolic compounds from lignin [9,10]
232 might results in a partial decomposition of those polymers, potentially changing the
233 arrangement of their functional groups, therefore causing shifts in the absorption bands

wavenumbers. The 3700 – 3000 cm^{-1} region of differential spectrum also varies from the one in extractives spectrum, suggesting that the changes in absorption upon extraction resulted not only from the direct –OH removal with extracted compounds, but rather that some rearrangement of the hydroxyl groups configuration in wood occurred as well.

The main change in wood upon its extraction was significant removal of the resin acids, represented by the 1697 cm^{-1} band [28] – the strongest band in extractives as well as in the differential spectrum. The shoulder on the 1697 cm^{-1} band corresponds to carbonyl C=O bond stretching in free fatty acids (1720-1706 cm^{-1}) and fatty acid esters (1750 – 1735 cm^{-1}) [29].

In the spectrum, there are also bands corresponding to –OH, $–CH_3$ and $–CH_2–$ groups at 3385, 2929 and 2868 cm^{-1}, respectively. Methylene scissoring and methyl asymmetrical bending are also represented by the 1457 cm^{-1} band and methyl symmetrical bending corresponds to the 1383 cm^{-1} band [29]. High intensity of those bands confirms the abundance of aliphatic chains in extracted compounds. The 1280 and 1240 cm^{-1} bands in the difference spectrum, as well as the 1250 cm^{-1} band in extractive spectrum, arise from single C-O bonds in carboxylic acids [30,31]. The 1166 cm^{-1} band in the difference spectra (1154 cm^{-1} in the extractives spectra) is most likely a result of C-O stretching in saturated fatty acid esters [29,30].

It can therefore be concluded, that typical pine extractives lipophilic compounds, namely free fatty acids, fatty acid esters and resin acids, were removed to some extent during the acetone extraction. It is also highly possible, that some of the observed C-O or OH stretching bands originate from triglycerides and phytosterols, that are also common wood extractives constituents. The presence of triglycerides was additionally indicated by the second peak of extractives decomposition DTG curve (*see section 3.4*). The two doublets at 1606, 1594 and 1512, 1497 cm^{-1} are characteristic of aromatic rings which suggests that some phenolic compounds were extracted from the pine wood as well.

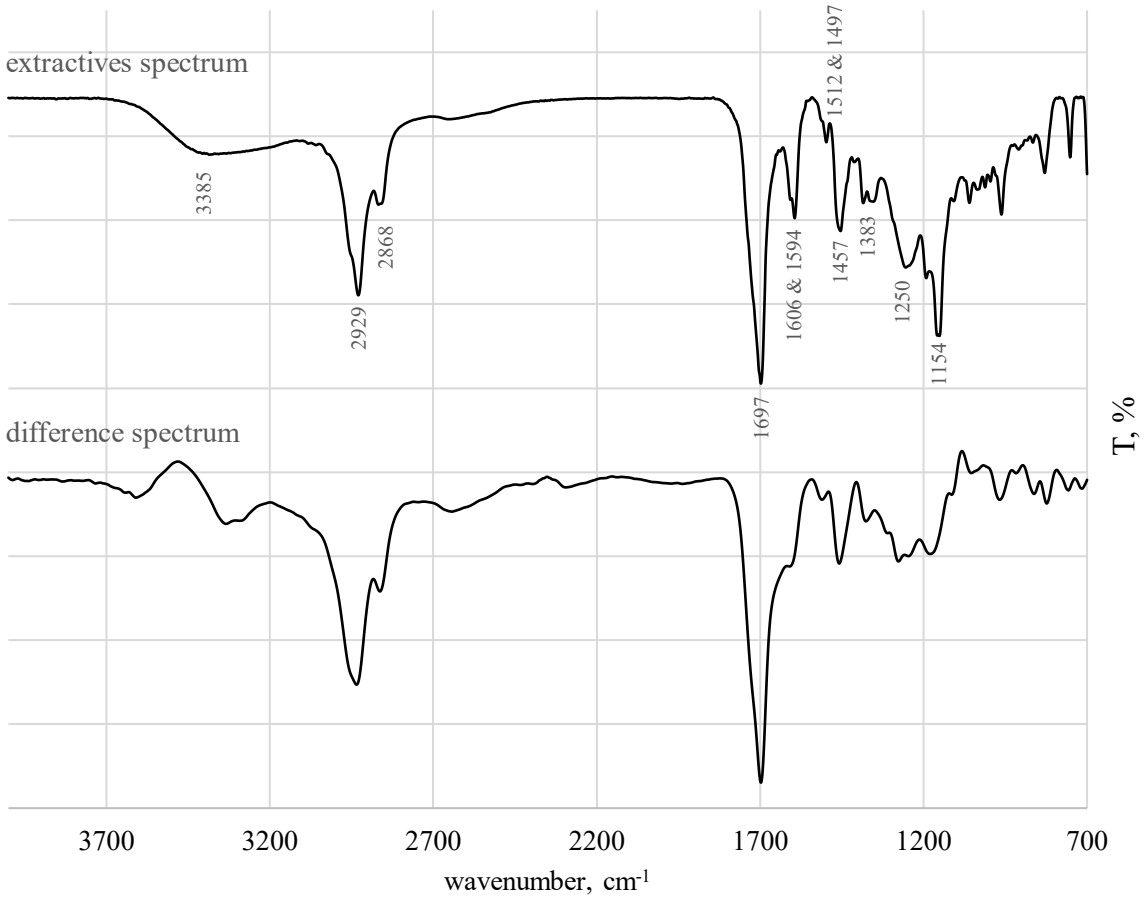

Fig. 1. FTIR spectrum of pine acetone extract film and the difference spectrum of extracted and non-extracted pine wood

3.2. Toluene pyrolytic conversion over pine char

Toluene conversion over both activated pine chars yielded some gaseous as well as some condensable by-products. Most likely, some solid residue in the form of coke was created as well, although it was not quantified in this study. Similar amounts of H_2 and CH_4 were detected in experiments with both chars, while no CO nor CO_2 were created. Yields of both gaseous products decreased with bed time-on-stream, until they fell below the detection limit

after about 20 min of the experiment. Analysis of the impinger bottles in both char experiments revealed the presence of benzene, as well as traces of ethylbenzene and xylenes along with the unreacted share of the fed toluene (Fig. 2).

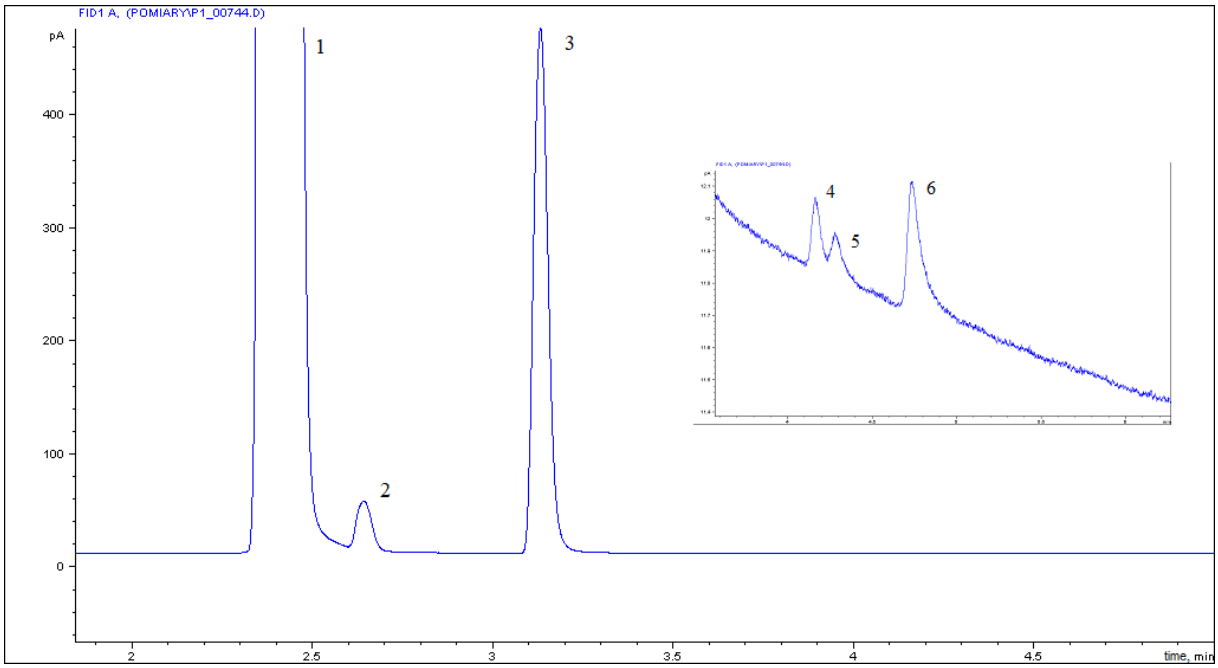

Fig. 2. Typical chromatogram for GD-FID analysis of impinger bottles content: 1 – dichloromethane, 2 – benzene, 3 – toluene, 4 – ethylbenzene, 5 – *m*-xylene/*p*-xylene, 6 – *o*-xylene

All condensable by-products yields were similar for both examined chars, with no significant differences according to the two-way ANOVA analysis. This suggests that the nature of toluene conversion pathways and the products selectivity did not changed when the extracted-pine char was used. A more detailed study of toluene conversion pathways and its products distribution is the scope of a future paper. Due to the lack of differences in the yields of the decomposition by-products, for the purpose of this work, only the toluene conversion was reported and expressed as:

$$\eta_T = (m_f - m_r)/m_f \quad (1)$$

where m_f is the mass of toluene fed to the reactor and m_r is the mass of toluene recovered in the impinger bottles. Toluene conversion, presented in Fig. 3, decreased with feeding time for both studied chars, due to their deactivation. However, the conversion was noticeably higher when extracted-pine activated char (PAE) was used. This observation was consolidated with two-way ANOVA analysis. The p-value for the comparison of PA and PAE series was 0.0049 << 0.05, suggesting that the difference between toluene conversions was significant. The improved performance of the PAE char was especially pronounced during the initial 30-40 min of toluene feeding. Prolonging the experiment resulted in similar conversions for both chars. Toluene conversions depicted in Fig. 3 are the total, summary conversions that include the highly efficient, initial decomposition. However, only 20 % of the toluene fed during the second 20 min of the experiment underwent conversion, for both tested chars. Negligibly small percentage (2 % for PA and 3 % for PAE) of toluene fed between 40th and 50th minute of the experiment was removed. Therefore, despite the improved initial toluene conversion, PAE char deactivation was reached at a similar time to PA char. Therefore, for the purpose of char characterisation, deactivated chars after 50 or 60 min of toluene pyrolysis were studied along with the fresh activated and non-activated chars.

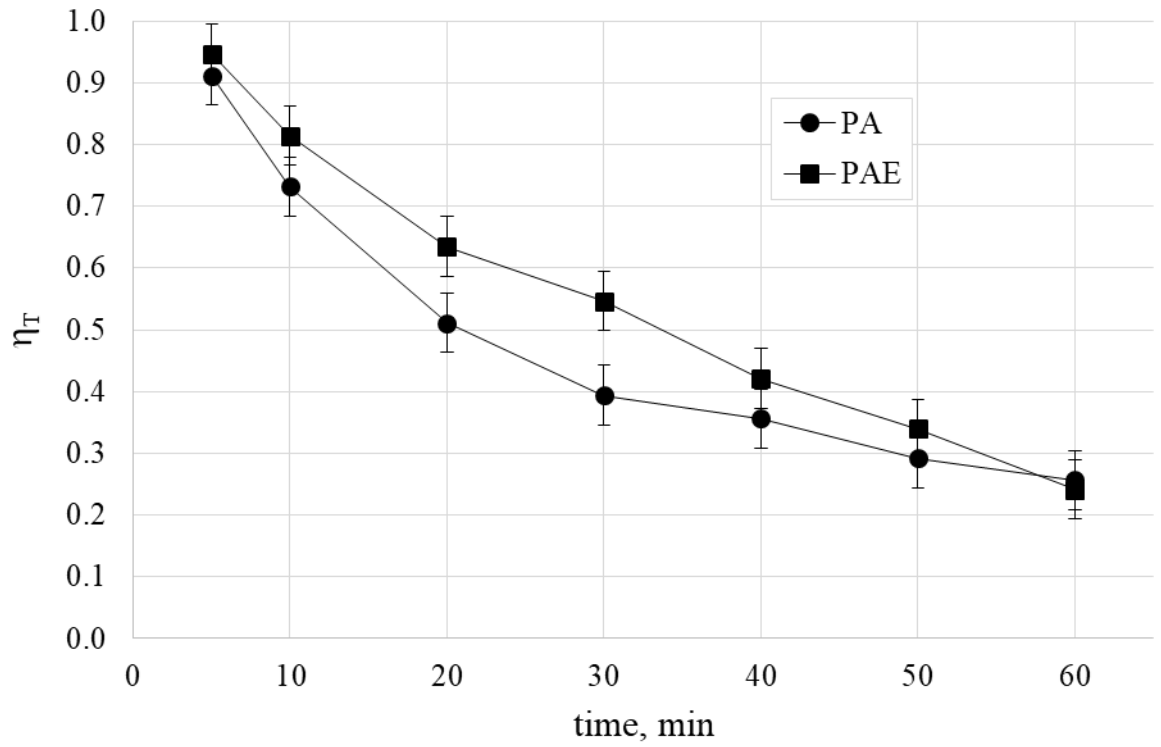

Fig. 3. Toluene pyrolytic conversion as a function of toluene feeding time for extracted (PAE) and non-extracted (PA) pine-derived activated chars

3.3. Char characterisation

Since the potential of chars for toluene removal changed upon raw biomass extraction, properties of both chars were studied in an attempt to determine the differences in the char structure caused by the lack of extractives during pyrolysis and following activation. Surface area and porosity, oxidative kinetics, surface chemistry and basic alkali and alkaline earth metals (AAEM) content analysis were applied to study the chars.

3.3.1. AAEM species

Na, K, Mg and Ca content in both chars was presented in Table 2. There was a significant spread of results due to a strong, intrinsic heterogeneity of the chars. Single-way ANOVA

315 analysis implied no significant differences in K and Ca content of both chars. Despite very
316 high RSD of the obtained data, the difference is expected to be significant for Na and Mg
317 concentrations (p=0.028 and p=0.021). However, Na content is negligibly small and Mg bears
318 the smallest catalytic effect among the studied metals [32]. Therefore, the correlation between
319 observed toluene conversion differences between the two chars and their AAEM composition
320 cannot be unambiguously confirmed. This assumption is supported by the results of an
321 oxidation kinetics experiment where despite slightly increased AAEM concentrations, PAE
322 has lower activation energy than PA char (*see section 3.3.3*).

323 Although acetone extraction is reported to remove some of the wood inorganics [10], the
324 significant loss of AAEM species due to volatilisation during pyrolysis and gasification of
325 biomass [33] is likely to overshadow the potentially diminished inorganics content after
326 extraction.

327

328 Table 2. Basic AAEM species content in non-extracted (PA) and acetone-extracted (PAE)
329 pine-derived, activated chars with relative standard deviations (RSD) of the measurements

	Na		**K**		**Mg**		**Ca**	
	mg/kg	RSD	mg/kg	RSD	mg/kg	RSD	mg/kg	RSD
PA	71.7	18.7%	1679.3	3.0%	810.05	2.9%	3615.12	4.3%
PAE	118.4	16.9%	1700.0	4.0%	885.49	3.0%	3908.98	4.6%

330

331 **3.3.2. Surface structure**

332 Surface area and pore volumes of pine chars before and after activation, as well as spent chars
333 after 50 min of toluene feeding are presented in Table 3. As expected, chars after pyrolysis
334 only, have significantly lower surface areas in comparison to the chars after steam activation.

335 Although total surface areas of P and PE chars were similar, extracted-pine derived char PE
336 had a significantly better developed microporous structure. The presence of extractives
337 increases solid products yield during pyrolysis. Therefore, it is likely that the enhanced char
338 creation in a constricted space of micropores reduced the micropores volume of the P char.
339 During activation, both total surface area and micropores area of P as well as PE more than
340 doubled. Activated char from extracted biomass, PAE, maintained a more microporous
341 structure than PA, although the difference in micropore area between extracted and non-
342 extracted wood chars decreased from 31.6 to 3.6 %. This suggests that the microporosity-
343 increasing effect of steam activation was overall more important than the initial influence of
344 the extraction. Nevertheless, the remaining difference in micropores area of PA and PAE
345 chars, caused by the extraction, is expected to be the main reason for increased conversion
346 over PAE char for the short toluene feeding times. Micropores are believed to greatly enhance
347 catalytic properties of activated chars, although they are also more easily sintered/deactivated.
348 Therefore, they play an important role only at the initial steps of catalytic conversion [2,34].
349 Since extraction of the feedstock resulted in an increased char performance for the initial 30
350 min, after which the efficiency of both chars became similar, spent chars, after 50 min toluene
351 feeding time, were analysed. Results showed that the surface areas decreased rapidly due to
352 char deactivation, and the initial difference in microporosity of PA and PAE disappeared. This
353 could provide an explanation for the similar performance of both chars after longer exposition
354 to toluene.

355 Steam activation is known to favour meso- and macropores creation, as opposed to CO_2
356 activation which mainly develops microporosity [35]. However, a dilution of steam and high
357 temperatures result in a pore structure more similar to those of CO_2 activated chars [36].
358 Using 15.5 vol.% steam in N_2 flow for 80 min resulted in an increase of meso and
359 macropores, which was an order of magnitude larger than the increase of micropores volume.

360 Nevertheless, a major part of the total surface area of char is due to micropores, proving their
361 importance in catalytic properties of the chars.

362 During toluene pyrolysis, both micro- as well as meso- and macropores volumes decreased,
363 although the relative depletion of microporosity was twice that of meso- and macropores
364 volume, supporting the theory of micropores importance and prompt deactivation at the
365 beginning of catalytic conversion processes.

366

367 Table 3. Surface area, micropores area, micropores volume and meso- and macropores
368 volume of fresh, activated (indicated with "A" in abbreviation) and non-activated chars
369 prepared form extracted (indicated with "E") and raw pine wood, as well as spent chars after
370 50 min run (indicated with "50")

	BET area m^2/g	**Micropores area, m^2/g**	**Micropores volume, cm^3/g**	**Meso- and macropores volume, cm^3/g**
P	244	182	0.068	0.003
PE	247	240	0.104	0.001
PA	668	503	0.222	0.092
PAE	686	521	0.230	0.089
PA_50	325	259	0.038	0.034
PAE_50	327	255	0.042	0.038

371

372 Changes in the char structure upon pyrolysis, activation and following deactivation in the
373 experiment with toluene can also be observed in the scanning electron micrographs. The non-
374 extracted pine char prepared during pyrolysis (Fig. 4a) had a relatively smooth surface with
375 "bubbles" resulting from the release of volatiles from the polymeric constituents that softened

upon heating [37]. During activation with steam, the char cracked and became uneven, while an abundance of small particles appeared on its surface (Fig. 4b). During the toluene conversion experiment, coke deposition as well as char thermal annealing removed the small labile particles and evened the surface to some extent, although the main, widest longitudinal cracks remained visible (Fig. 4c).

a)

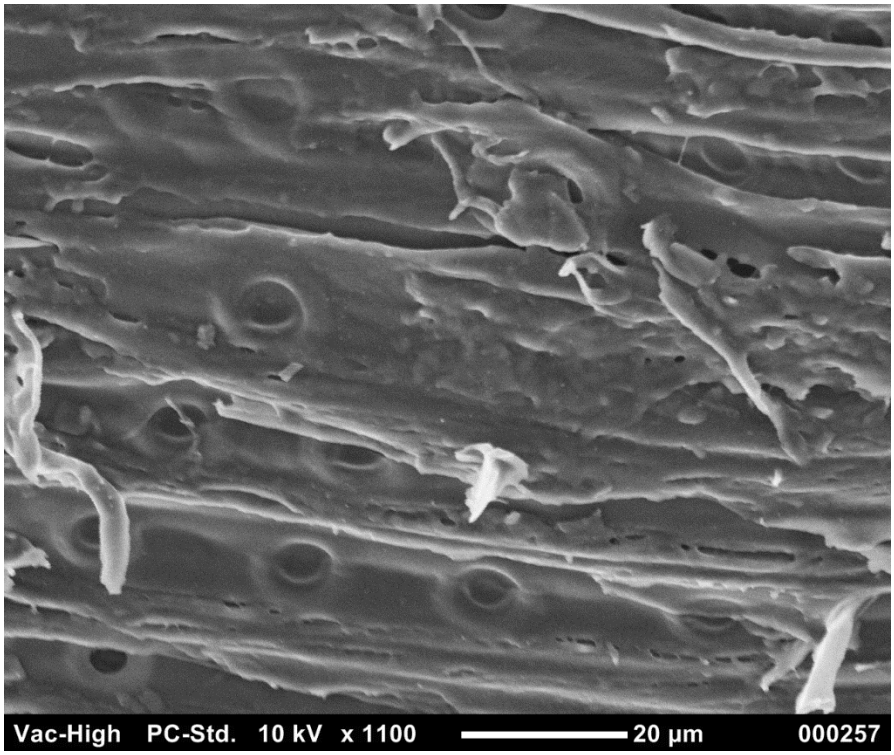

b)

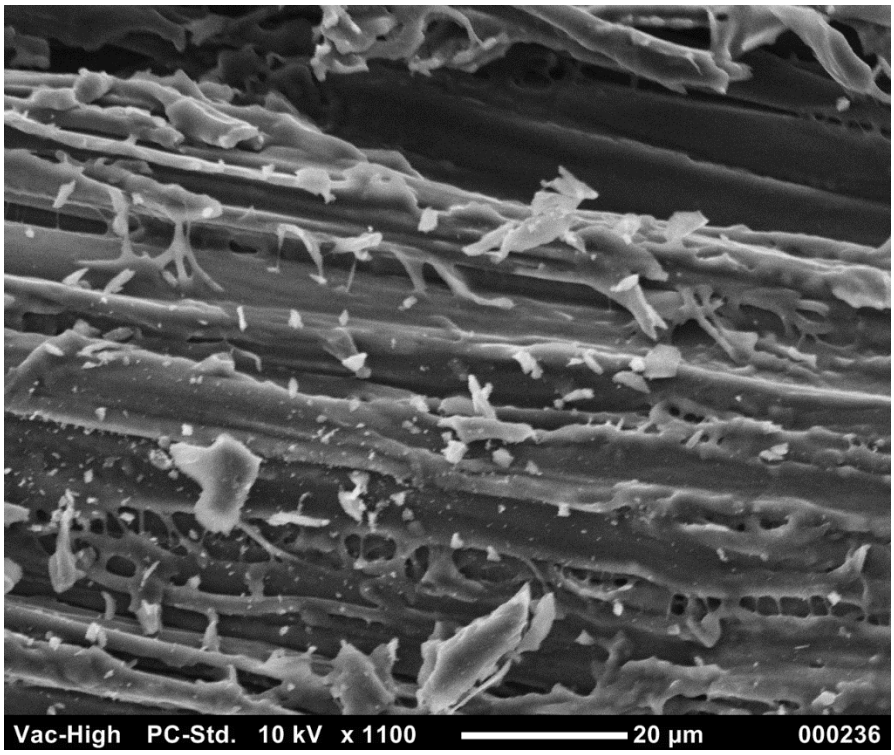

c)

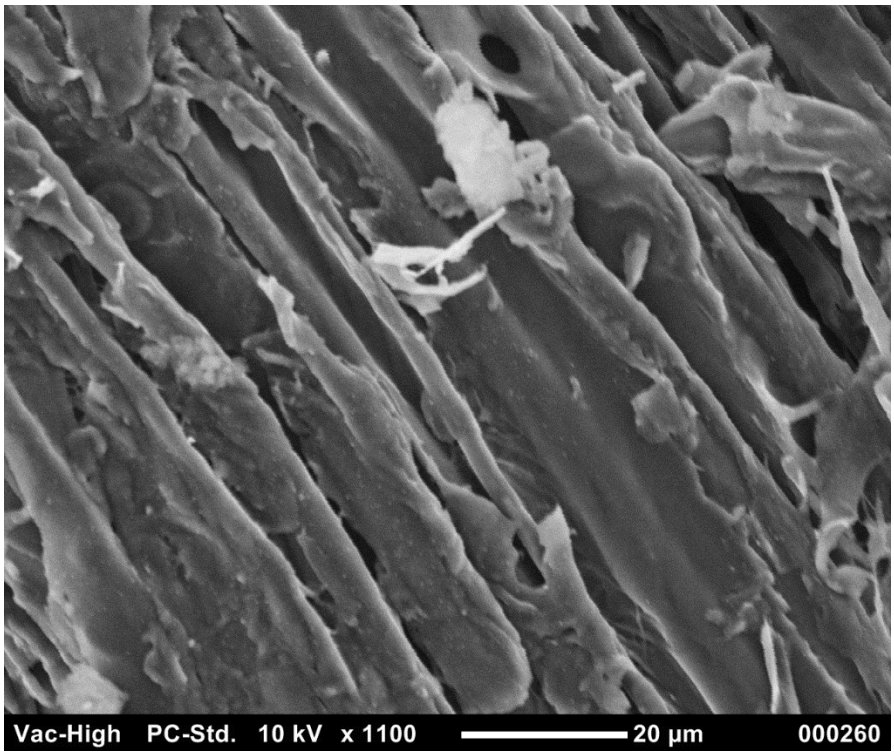

Fig. 4. Scanning electron micrographs of non-extracted pine char a) before the activation (P), b) after steam activation (PA), c) after 40 min time-on-stream in toluene conversion experiments (PA_40)

3.3.3. Char oxidation kinetics

The activation energies (E_a) of the selected chars oxidation for the mass loss in the region of 3 – 10 % of the initial sample mass as well as the corresponding temperature zones were presented in Table 4. Both non-activated chars had similar activation energies. After activation with steam, E_a almost doubled and the oxidation was shifted to higher temperatures. Increase in E_a and reaction temperatures can be explained by partial gasification of the chars occurring during the activation process, when some more volatile species are released from the chars. Although oxidation of both PA and PAE samples occurred at similar temperatures, the E_a of the extracted sample was slightly higher. Chars deactivated after 60 min of toluene pyrolysis had slightly increased E_a values and oxidation temperatures. Deactivated char from extracted pine PAE_60 maintained slightly lower reactivity in comparison to non-extracted pine char PA_60. Diminished reactivity of spent chars can be explained by the inhibiting effect of coke deposition on char surfaces.

The differences between extracted and non-extracted pine char oxidation kinetics arise after the steam activation. It is possible, that the microporosity of non-activated chars does not play a significant role during TGA runs with oxygen, thus the similar E_a values for P and PE, yet it affects the steam activation process, resulting in a slightly lower E_a value of PA in comparison to PAE char. Therefore, there are differences in the effects the extraction has on the char oxidation, depending on the oxidation process characteristics. The lack of the extraction influence during TGA oxidation of non-activated chars and the presence of this influence during char activation in the reactor, might be the result of different oxidising agents as well as due to different temperature profiles. TGA kinetics were studied for the initial decomposition starting at relatively low temperatures, whereas steam activation started while the chars were already heated to 800 °C. The 15-16 kJ/mol difference in E_a values between extracted and non-extracted samples is maintained after deactivation of chars, despite the

414 vanishing differences in surface area and porosity of the spent chars (*see section 3.3.2*). Char
415 oxidation kinetic in the relative abundance of oxygen (12 vol.%) is most likely less sensitive,
416 compared to toluene pyrolytic conversion, to diffusional constrictions caused by char surface
417 structure. Therefore, the activation energies obtained from TGA experiments does not exhibit
418 correlation with porosity development/decrease.

419

420 Table 4. Activation energies E_a obtained from TGA experiment on chars oxidation, calculated
421 for the 3 – 10 % mass loss range as well as the initial t_i and final t_f temperatures of the
422 studied mass loss regions

	E_a	t_i	t_f
	kJ/mol	°C	°C
P	77	394	452
PE	80	392	447
PA	143	433	470
PAE	159	440	472
PA_60	169	448	479
PAE_60	184	454	482

423

424 **3.3.4. FTIR of pine chars**

425 The spectra of extracted and non-extracted chars, presented in Fig. 5, bear strong resemblance
426 to each other, suggesting similar chemical structures and behaviour upon activation and
427 following deactivation.

428 The FTIR spectra of prepared chars can be divided into several sections, corresponding to the
429 characteristic bonds in the surface compounds [38,39]. The C-H bonds in aromatic structures

absorb in the region of 900 – 700 cm^{-1}, depending on the substitution pattern of the ring. Numerous small bands that can be observed within this region suggest a big variety of ring substituents present within the aromatic rings of the char matrix. Other regions characteristic for aromatic structures are 1625 – 1575 and 1525 – 1440 cm^{-1}, where in the case of a single compound, there are usually doublet bands in each of those regions. In the case of highly complex and diversified char structures, only the general increase of absorption for those wavelengths can be observed, providing confirmation of the aromatic character of the chars.

The wide band between 1625 – 1450 cm^{-1} encompasses both regions characteristic for aromatic rings. A plausible explanation for high absorption between those regions, i.e. 1575 – 1525 cm^{-1}, is that large polycyclic structures absorb abundantly within the 1625 – 1450 cm^{-1} region, as can be suggested by the calculations performed by Pathak and Rastogi [40].

Other significant absorption regions correspond to C=O and C-O bonds in various configurations in char surface groups. The carbonyl group absorption wavelength strongly depends on the bonds in the approximate vicinity to the C=O bond. Therefore, carbonyl stretching can absorb from 1680 cm^{-1} for aromatic carboxylic acids, through around 1700 cm^{-1} for ketones, and up to 1800 cm^{-1} for some esters, lactones and acid anhydrides. The wide band within the 2000 – 1660 cm^{-1} region, that can be observed in Fig. 5, is most likely the result of various C=O structures on the char surface, as well as some overtones of aromatic ring bonds. The region of 1310 – 1000 cm^{-1} is generally assigned to C-O-C stretching in ethers, C-O stretching in esters and lactones and C-C(=O)-C bending in ketones.

Phenolic groups are yet another plausible structure on the char surface (confirmed further by Boehm titration, *see section 3.3.5*). Characteristic absorption bands for phenolic C-O stretch appear at 1260 – 1180 cm^{-1} and the O-H in-plane bending occurs at 1390-1330 cm^{-1}. Absorption within the 1000 – 900 cm^{-1} region can be attributed to the C-O-C stretch in acid

454 anhydrides as well as C-C stretches of the carbon matrix that absorb within the whole
455 fingerprint region.

456 The lack of absorption at certain regions of registered spectra can serve as a confirmation of
457 the absence of certain surface structures of the chars. Since no evident bands were registered
458 at 3000 – 2800 and 2260-2100 cm^{-1}, it can be assumed that no alkynes and no significant
459 amount of aliphatic structures in general, are present in either of the chars.

460 The char spectra obtained in this study correlate well with the results reported so far [41,42].
461 The general structure of all the char spectra does not differ much. This suggests similar
462 structures of chars, that are a highly aromatic carbon matrix with some oxygen functional
463 groups and a lack of significant aliphatic structures. However, it can be noticed, that the
464 activation of char increased the intensity of all registered bands, suggesting the creation of
465 new oxygenates upon reaction with steam. Toluene pyrolysis over activated char resulted in
466 its progressive deactivation. The spent char spectrum resembles the initial, pre-activation one.
467 This suggest the existence of a memory effect of char upon the deactivation as well as
468 similarity in the structure of non-activated wood char and toluene-derived, deposited coke.
469 There is also a visible change in the relative intensity of absorption within 1460 – 1340 cm^{-1}
470 as well as 1300 – 1130 cm^{-1} region. While in the non-activated and activated samples, there is
471 a clear, single band at 1374 and 1231 cm^{-1}, in the activated char those bands appear as
472 shoulders within the high absorption of the whole regions. This observation might suggest a
473 more uniform structure of char in relation to the bonds absorbing at these wavelengths. Since
474 phenolic O-H and C-O bonds absorb at 1390 – 1330 and 1260 – 1180 cm^{-1}, respectively, and
475 the single remaining bands in the non-activated chars correspond particularly well with the
476 pure phenol spectrum [39], it is possible that phenolic groups on the non-activated char are
477 mainly attached to aromatic rings with no other functionalities within their immediate vicinity

478 and, upon activation, some adjacent oxygen compounds are created, resulting in more spread
479 absorption bands.

480 In the non-activated char spectra, a small difference can be distinguished between extracted
481 and non-extracted pine chars in the shape of the wide 1150 – 900 cm^{-1} absorption band. In the
482 P char spectrum, the intensity of the left shoulder of the band is lower than the right one,
483 while in the PE spectrum the band is more symmetrical. This might suggest a different
484 distribution of C-O functionalities in non-activated chars. There is however no visible
485 difference between both chars after activation and following deactivation.

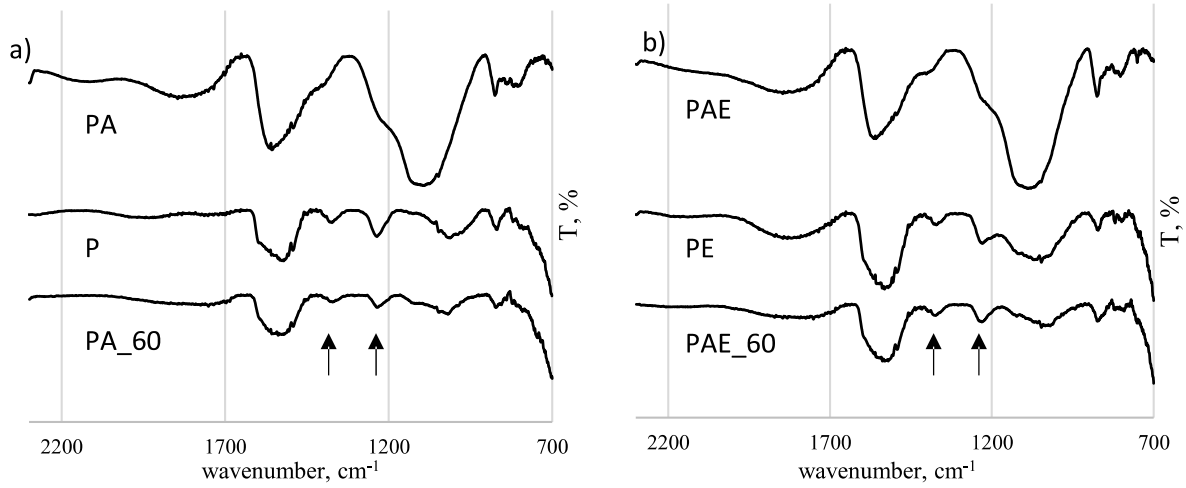

486

487 Fig. 5. FTIR spectra of the activated (abbreviated with "A") and non-activated chars from a)
488 non-extracted and b) extracted (abbreviated with "E") pine, as well as spent chars after 60 min
489 time-on-stream in toluene conversion experiment (abbreviated with "60"); arrows indicate
490 1374 and 1231 cm^{-1} bands; since no bands were registered at higher wavenumbers, only the
491 2200 – 700 cm^{-1} region is presented

492 **3.3.5. Acidic sites on activated chars surfaces**

493 The acidic sites distribution obtained from the Bohem titration are presented in Table 5. The
494 amount of the weakest acidic sites, i.e. phenolic groups, was very similar for both activated
495 chars. There were small differences in the lactonic and carboxylic groups. Total acidity of

496 chars was therefore equal to 0.275 and 0.298 meq/g for PA and PAE chars, respectively.
497 These values correspond well with literature data, especially since the amount of acidic sites
498 decreases with char preparation temperature [26,43,44]. The chars, prior to activation had
499 significantly less acidic sites, with a total acidity of 0.103 and 0.148 meq/g for P and PE,
500 respectively. Upon oxidation with steam, there was an increase in all three acidic site types.
501 The char from non-extracted pine initially, after the pyrolysis step, had notably higher acidity,
502 mainly due to the carboxylic groups content. After the activation, the difference between the
503 chars diminished.

504 Similar acidic sites distribution on the char surfaces correlates well with the similar surface
505 chemistry characteristics obtained from FTIR spectral analysis. The changes in the spectrum
506 of non-activated/deactivated and activated chars (indicated in Fig. 5 by arrows) can result
507 from the creation of some new carboxylic and lactonic functionalities in the vicinity of
508 existing phenolic groups upon reaction with steam. Significantly higher carboxylic groups
509 content in PE, in comparison to P char, might be responsible for the observed difference
510 between 1150 – 900 cm^{-1} band shapes of P and PE spectra (Fig. 5).

511

512 Table 5. Acidic sites distribution on chars surfaces, determined by Boehm titration (activated
513 chars abbreviated with “A”, extracted-pine chars abbreviated with “E”)

	Carboxylic groups, meq/g	Lactonic groups, meq/g	Phenolic groups, meq/g
P	0.048	0.017	0.038
PE	0.113	-0.008	0.043
PA	0.149	0.057	0.069
PAE	0.188	0.045	0.065

514

515 **3.4. Thermogravimetric analysis of pine pyrolysis**

516 Initially, TGA experiments were carried out in N_2 flow at a heating rate of 10 °C/min. First
517 derivatives of a pyrolytic mass loss of extracted and raw pine wood are shown in Fig. 6a.
518 Moreover, the mass loss curves are also provided in Fig. 6c-d to show the mass loss range of
519 the samples. Derivatives were further deconvoluted using Gaussian distribution (R^2>0.99).
520 The extracted pine derivative curve consists of three peaks, corresponding to the main
521 polymeric constituents in woody biomass – hemicellulose, cellulose and lignin, peaking at
522 343, 377 and 419 °C, respectively (Fig. 7a). In the extractives decomposition curve, three
523 peaks can be distinguished at 147, 305 and 450 °C. In DTG of non-extracted pine pyrolysis,
524 both the main polymers and extractive compounds can be observed (Fig. 7c). Hemicellulose
525 and cellulose decomposition peak temperatures and intensities are similar for raw and
526 extracted samples. The maximum mass loss rate for hemicellulose and cellulose (on an
527 extractive-free mass basis) equals -0.537 and -0.673 %/°C for raw and -0.531 and -
528 0.675 %/°C for extracted pine, respectively. This suggests that holocellulose decomposition
529 was unaffected by the presence of extractives in the sample. The lignin peak however, is
530 narrower and occurs at a lower temperature (419 °C) in the extracted sample, as compared to
531 the raw material (491 °C). The shift in the lignin peak might be explained by some changes in
532 lignin structure resulting from the extraction, especially since FTIR analysis confirmed the
533 removal of some phenolic compounds from pine (*see section 3.1*).

534 The DTG curve of pine extractives (Fig. 7c) bears resemblance to that of ethanol extractives
535 from Mongolian pine reported by Guo et al. [14] as well as cashew nut-shell liquid (from
536 mechanical extraction of cashew nut shells) presented by Melzer et al. [45]. The low
537 temperature peak might be the result of decarboxylation of acids or release of some more
538 volatile terpenes and ketones. Free fatty acids and fatty acid methyl esters, on the other hand,

539 are reported to thermally decompose in a single step, with a main mass loss rate at a
540 temperature region of 160 – 370 °C [45,46]. Pyrolysis rates for resin acids also peak at around
541 300 °C [47]. Therefore, the main extractives peak registered in this study might be caused by
542 aliphatic chain degradation in acids and acid esters [45,46,48].

543 Triglycerides are reported to decompose in two steps – the first one corresponding to acid
544 chain decomposition. The second step is recognised as glycerol decomposition [45,46,49],
545 which is most likely the origin of the small peak at 450 °C, registered in this study as well.

546 Since the heating rate during pyrolysis in the quartz tube reactor was significantly higher than
547 the one applied in the TGA studies, additional TGA runs at 50 °C/min were performed.
548 Because of the increased overlapping of wood pseudo components and extractives peaks, no
549 straightforward DTG deconvolution could be performed. It could be seen however, as
550 presented in Fig. 6, that at the 10 °C/min heating rate, DTG curves at temperatures above 280
551 °C have similar shapes for both, extracted and non-extracted pine, with the only difference in
552 the maximum decomposition rate that was achieved. At 50 °C/min, not only is the extracted
553 pine DTG peak higher, but the whole slope of the derivative up to the temperature of
554 maximum decomposition, differs significantly from that of a non-extracted pine. This
555 suggests that during high heating rate pyrolysis, the presence of extractives changes the
556 overall kinetics of biomass conversion and extractives volatilisation likely interferes with
557 polymeric constituents decompositions.

558 Some crosslinking reactions were observed by Jandura et al. [50] during esterified cellulose
559 pyrolysis. The magnitude of the exothermic reaction assigned to crosslinking was especially
560 high with cellulose esterified with unsaturated fatty acids, suggesting some interaction
561 between chain double bonds and decomposing cellulose, especially since the activation
562 energy of double bonds and that of the thermal initiation of free radicals from cellulose
563 decomposition are reported to be similar. Since pine extractives are abundant in unsaturated

fatty acids [11], it is possible that some crosslinking reactions occur between extractives and polymeric constituents of wood during pyrolysis.

The influence of extractives on cellulose decomposition was already reported by Guo et al. [14], who performed pyrolysis of Mongolian pine at a heating rate of 40 °C/min, and established that extracted pine pyrolysis yields more inorganic species like H_2O, CO and CO_2, and less organic acids. Since cellulose decomposition occurs in two competing pathways – either to acetic acid or to levoglucosan followed by its further decomposition to CO_2 and water, they concluded that the presence of extractives in wood during the pyrolysis favours acetic acid creation. It is also reported that removal of inorganic species due to extraction might decrease the catalytic affinity towards char formation [8].

Besides possible chemical interactions between biomass constituents, some physical constrictions during pyrolysis are also expected. Extractives are reported to create a layer covering wood fibres that inhibits volatile species evolution, increasing residence times within the particle and enhancing secondary tar reactions resulting in increased char yield at the expense of liquid products [17–19,51].

Suppression of polymer devolatilisation by the extractives layer is a plausible explanation for the significant differences in extracted (PE) and non-extracted (P) pine char pore distributions. Increased secondary reactions and enhanced char formation will most likely occur in constricted spaces, i.e. micropores, leading to a less developed microporosity in the P char.

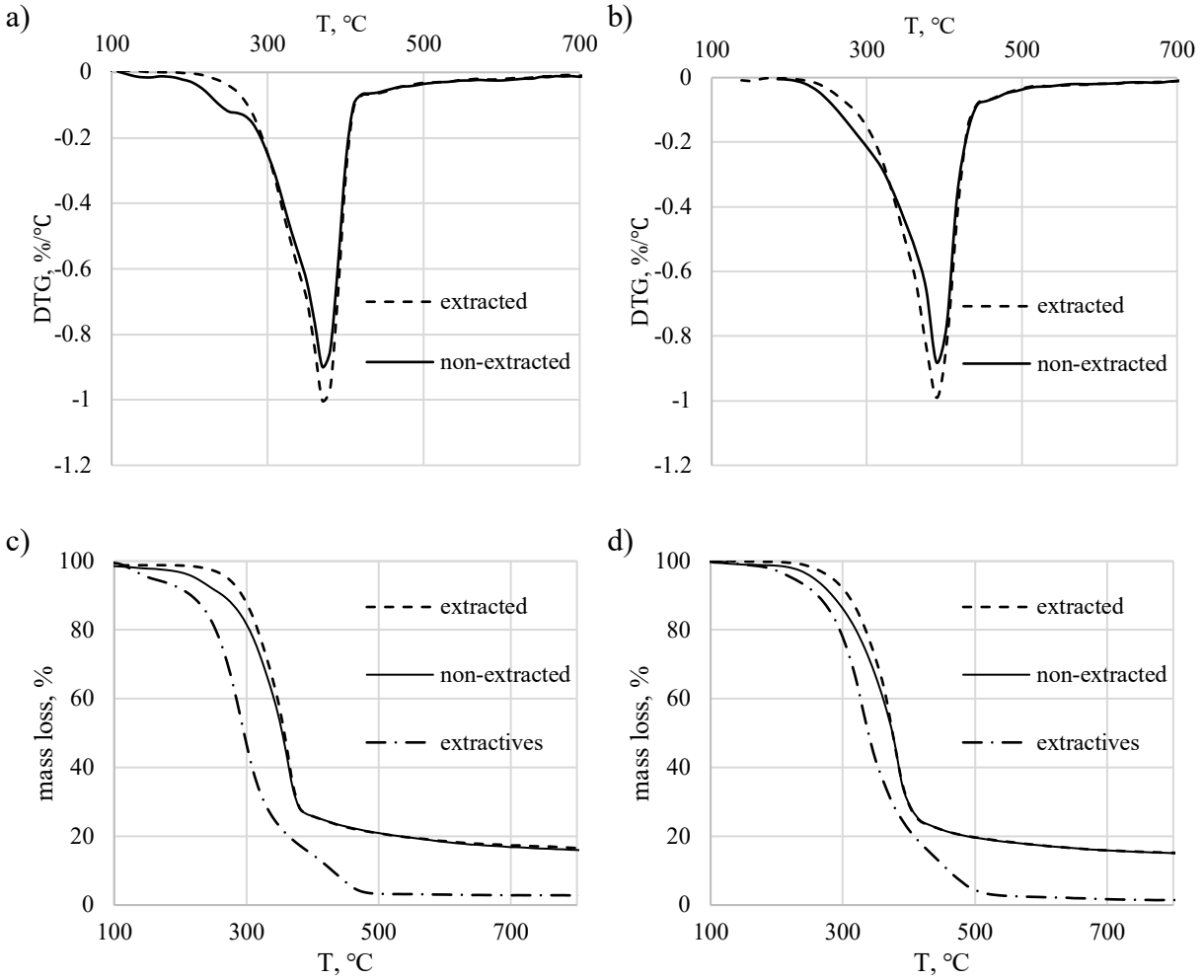

Fig. 6. First derivatives DTG and mass loss curves of extracted and non-extracted pine wood obtained from TGA pyrolysis experiments at a), c) 10 °C/min and b), d) 50 °C/min heating rate

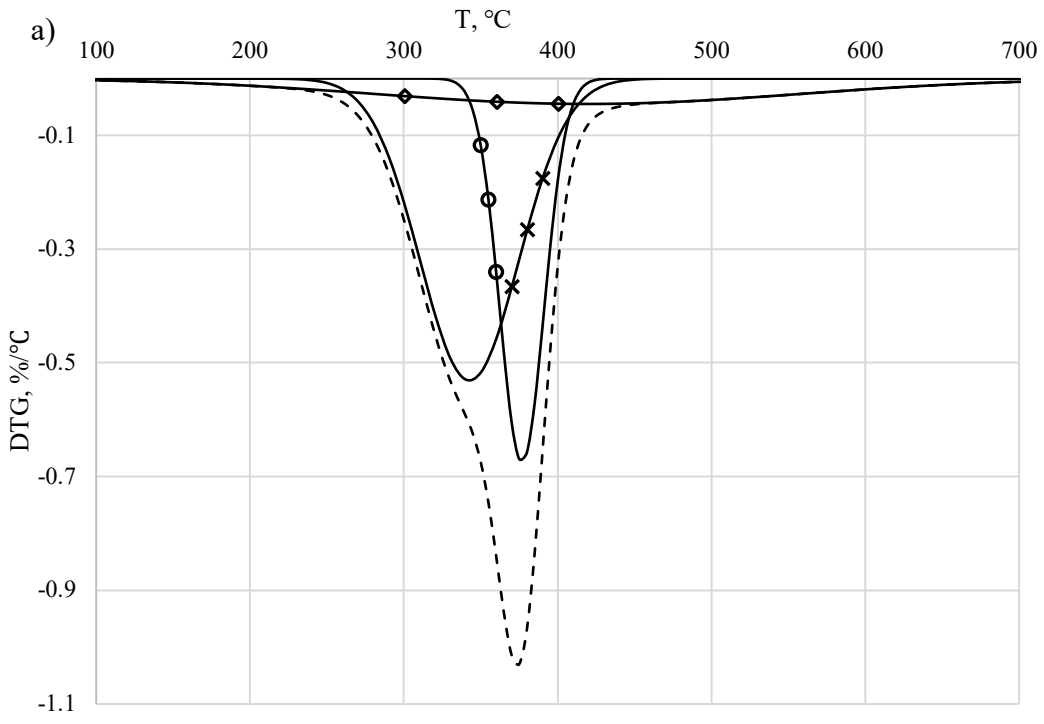
a)
T, °C
100
200
300
400
500
600
700
-0.1
-0.3
-0.5
-0.7
-0.9
-1.1
DTG, %/°C

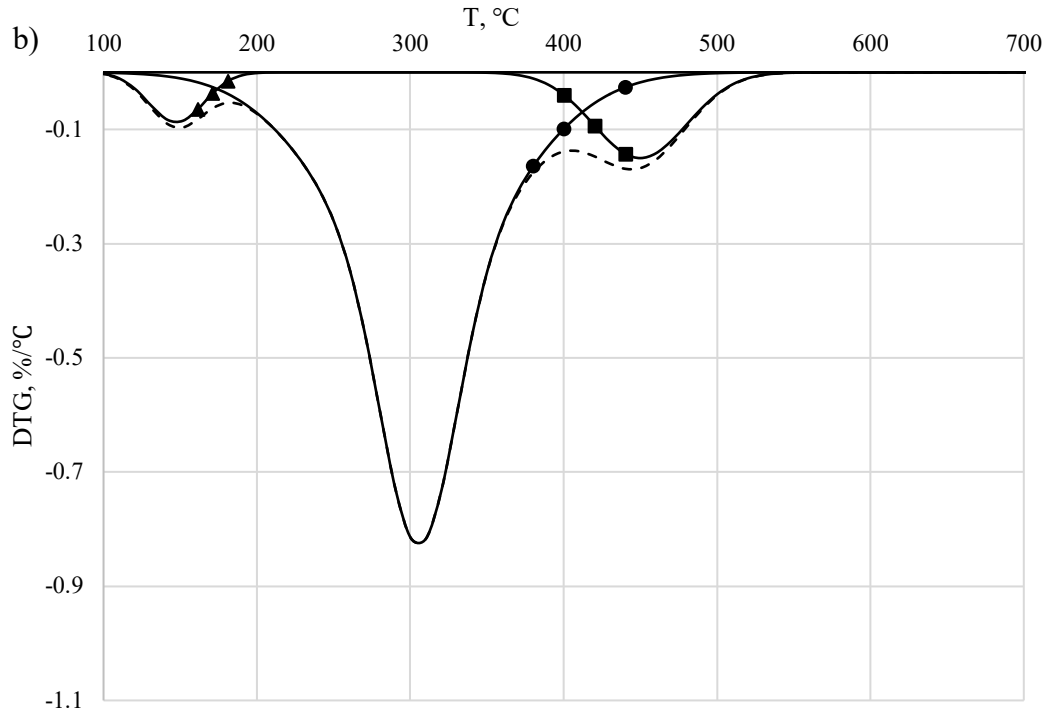
b)
T, °C
100
200
300
400
500
600
700
-0.1
-0.3
-0.5
-0.7
-0.9
-1.1
DTG, %/°C

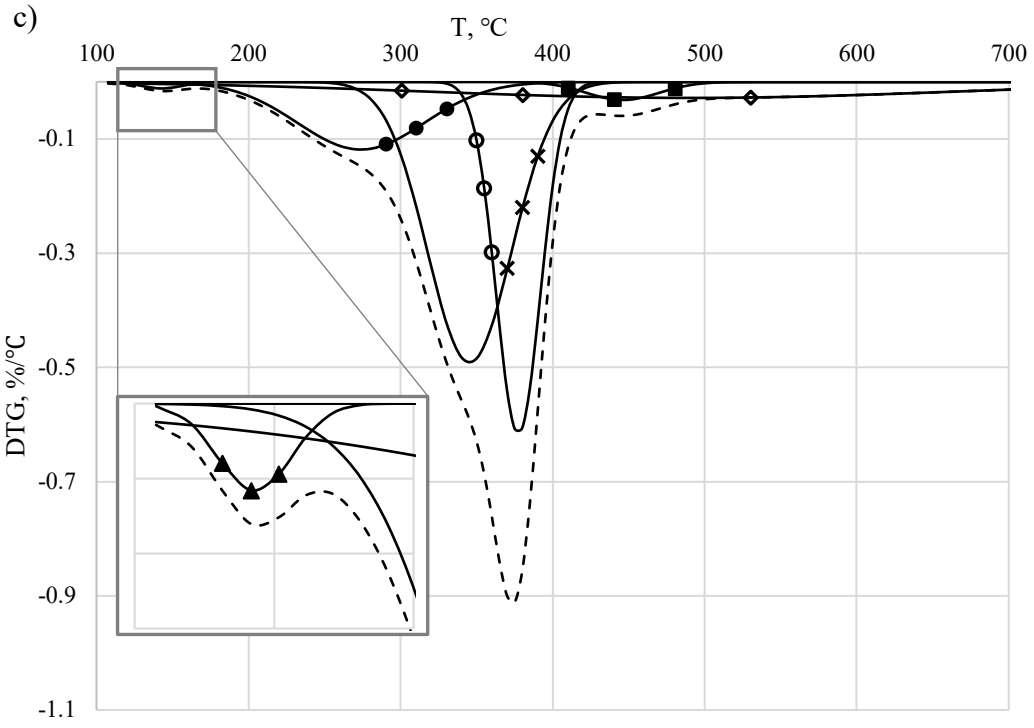

Fig. 7. Deconvolution of DTG curves of a) extracted pine b) acetone extracted compounds and c) non-extracted pine pyrolytic decomposition at 10 °C/min heating rate using Gaussian functions to represent × – hemicellulose, ○ – cellulose, ◇ – lignin and ▲, ●, ■ – 1st, 2nd, 3rd extractives compounds, respectively

4. Conclusions

In this paper, acetone-extracted and raw pine wood was used to create steam activated char. Obtained materials were then tested for their affinity towards high temperature pyrolytic removal of toluene. Char performance was then discussed in relation to their properties, i.e. porosity and surface chemistry.

The following conclusions were drawn based on the obtained results:

604 • Although it was mainly volatile compounds that were extracted from pine, their
605 removal influenced the pyrolysis of wood, significantly changing the microporosity,
606 and to some extent the acidity, of derived chars.
607 • The effect of extraction on pore distributions was diminished during the steam
608 activation process but extracted-wood derived char maintained a slightly more
609 microporous structure. This resulted in an enhanced catalytic performance in the initial
610 stage of the toluene conversion experiment. Micropores sintering during toluene
611 conversion led to similar pore distributions in the spent chars after 50 min of exposure,
612 which is in accordance to the similar toluene conversion rates achieved by both chars
613 at this point of the experiment.
614 • The initial advantage in acidic site distributions of the extracted pine char diminished
615 during activation, yet there was still a small difference in carboxylic groups content of
616 PA and PAE chars.
617 • Since extraction had no visible effect on TGA oxidation runs of fresh non-activated
618 chars (P and PE), but had an impact on oxidation during steam activation, it can be
619 expected that the behaviour of extracted and non-extracted chars is strongly related to
620 oxidation process parameters like the temperature program or the nature of the
621 oxidising agent.
622 • The comparison of lower and higher heating rate pyrolysis of pine wood as well as the
623 changes to the microporosity and the acidity differences between the chars prior to and
624 during steam activation, suggests that the effect of extractives removal is strongly
625 correlated to the pyrolysis heating rate and to the following char activation time.
626 Therefore, more future studies of these relations are advised.

627 Performed studies suggest that the presence of extractives in the feedstock for biochar
628 preparation can influence the properties of the derived product. The effect occurs alongside

the impact of other char preparation parameters, e.g. feedstock nature, pyrolysis and activation conditions. Moreover, the magnitude of the effect of the extractives will depend on the thermochemical treatment conditions.

Acknowledgements

This work was supported by the National Science Centre, Poland (project PRELUDIUM 10 number UMO-2015/19/N/ST8/02454). The thermogravimetric analysis of pine chars and scanning electron micrographs were financed by the School of Engineering, University of Lincoln. Authors would also like to express their gratitude to Mr Krzysztof Rajczykowski for performing AAEM content analysis and to Mr Philip Staton for the assistance with obtaining scanning electron micrographs.

References

[1] L. Burhenne, T. Aicher, Benzene removal over a fixed bed of wood char: The effect of pyrolysis temperature and activation with CO2 on the char reactivity, Fuel Process. Technol. 127 (2014) 140–148. doi:10.1016/j.fuproc.2014.05.034.

[2] F. Nestler, L. Burhenne, M.J. Amtenbrink, T. Aicher, Catalytic decomposition of biomass tars: The impact of wood char surface characteristics on the catalytic performance for naphthalene removal, Fuel Process. Technol. 145 (2016) 31–41. doi:10.1016/j.fuproc.2016.01.020.

[3] S. Hosokai, K. Kumabe, M. Ohshita, K. Norinaga, C.Z. Li, J. ichiro Hayashi, Mechanism of decomposition of aromatics over charcoal and necessary condition for maintaining its activity, Fuel. 87 (2008) 2914–2922. doi:10.1016/j.fuel.2008.04.019.

[4] D. Fuentes-Cano, A. Gómez-Barea, S. Nilsson, P. Ollero, Decomposition kinetics of model tar compounds over chars with different internal structure to model hot tar removal in biomass gasification, Chem. Eng. J. 228 (2013) 1223–1233. doi:10.1016/j.cej.2013.03.130.

[5] Y. Song, J. Xiang, S. Hu, D.M. Quyn, Y. Zhao, X. Hu, Y. Wang, C.Z. Li, Importance of the aromatic structures in volatiles to the in-situ destruction of nascent tar during the volatile-char interactions, Fuel Process. Technol. 132 (2015) 31–38. doi:10.1016/j.fuproc.2014.12.035.

[6] G. Ravenni, Z. Sárossy, J. Ahrenfeldt, U.B. Henriksen, Activity of chars and activated carbons for removal and decomposition of tar model compounds – A review, Renew. Sustain. Energy Rev. 94 (2018) 1044–1056. doi:10.1016/J.RSER.2018.07.001.

[7] R.W. Hemingway, W.E. Hillis, Changes in fats and resins of Pinus radiata associated with heartwood formation, APPITA. 24 (1971) 439–443.

[8] G. Várhegyi, M.G. Grønli, C. Di Blasi, Effects of Sample Origin, Extraction, and Hot-Water Washing on the Devolatilization Kinetics of Chestnut Wood, Ind. Eng. Chem. Res. 43 (2004) 2356–2367. doi:10.1021/ie034168f.

[9] E. Mészáros, E. Jakab, G. Várhegyi, TG/MS, Py-GC/MS and THM-GC/MS study of the composition and thermal behavior of extractive components of Robinia pseudoacacia, J. Anal. Appl. Pyrolysis. 79 (2007) 61–70. doi:10.1016/j.jaap.2006.12.007.

[10] B. Holmbom, E. Sjostrom, R. Alèn, Analytical methods in wood chemistry, Pulping Papermak. 125 (1999).

[11] R.W. Hemingway, W.E. Hillis, L.S. Lau, The extractives of Pinus pinaster wood, 1973.

675 [12] D.F. Zinkel, Fats and Fatty Acids BT - Natural Products of Woody Plants: Chemicals
676 Extraneous to the Lignocellulosic Cell Wall, in: J.W. Rowe (Ed.), Springer Berlin
677 Heidelberg, Berlin, Heidelberg, 1989: pp. 299–304. doi:10.1007/978-3-642-74075-
678 6_10.

679 [13] A. Gutiérrez, J.C. del Río, F.J. González-Vila, F. Martín, Analysis of lipophilic
680 extractives from wood and pitch deposits by solid-phase extraction and gas
681 chromatography, J. Chromatogr. A. 823 (1998) 449–455.
682 doi:http://dx.doi.org/10.1016/S0021-9673(98)00356-2.

683 [14] X. Guo, S. Wang, K. Wang, Q. Liu, Z. Luo, Influence of extractives on mechanism of
684 biomass pyrolysis, J. Fuel Chem. Technol. 38 (2010) 42–46. doi:10.1016/S1872-
685 5813(10)60019-9.

686 [15] A.N. Shebani, A.J. van Reenen, M. Meincken, The effect of wood extractives on the
687 thermal stability of different wood species, Thermochim. Acta. 471 (2008) 43–50.
688 doi:10.1016/j.tca.2008.02.020.

689 [16] C.-Y. Hse, M.-L. Kuo, Influence of extractives on wood gluing and finishing-a review,
690 For. Prod. J. 38 (1988) 52–56.

691 [17] C. Roy, H. Pakdel, D. Brouillard, The role of extractives during vacuum pyrolysis of
692 wood, J. Appl. Polym. Sci. 41 (1990) 337–348. doi:10.1002/app.1990.070410126.

693 [18] C. Di Blasi, C. Branca, A. Santoro, E. Gonzalez Hernandez, Pyrolytic behavior and
694 products of some wood varieties, Combust. Flame. 124 (2001) 165–177.
695 doi:10.1016/S0010-2180(00)00191-7.

696 [19] C. Di Blasi, C. Branca, A. Santoro, R.A. Perez Bermudez, Weight loss dynamics of
697 wood chips under fast radiative heating, J. Anal. Appl. Pyrolysis. 57 (2001) 77–90.

doi:10.1016/S0165-2370(00)00119-4.

[20] A. Korus, A. Samson, A. Szlęk, A. Katelbach-Woźniak, S. Sładek, Pyrolytic toluene conversion to benzene and coke over activated carbon in a fixed-bed reactor, Fuel. 207 (2017). doi:10.1016/j.fuel.2017.06.088.

[21] J.P.A. Neeft, Rationale for setup of impinger train, SenterNovem CEN BT/TF. 143 (2005) 1–14.

[22] L. Burhenne, M. Damiani, T. Aicher, Effect of feedstock water content and pyrolysis temperature on the structure and reactivity of spruce wood char produced in fixed bed pyrolysis, Fuel. 107 (2013) 836–847. doi:10.1016/j.fuel.2013.01.033.

[23] S.L. Goertzen, K.D. Thériault, A.M. Oickle, A.C. Tarasuk, H.A. Andreas, Standardization of the Boehm titration. Part I. CO2 expulsion and endpoint determination, Carbon N. Y. 48 (2010) 1252–1261. doi:10.1016/j.carbon.2009.11.050.

[24] A.M. Oickle, S.L. Goertzen, K.R. Hopper, Y.O. Abdalla, H.A. Andreas, Standardization of the Boehm titration: Part II. Method of agitation, effect of filtering and dilute titrant, Carbon N. Y. 48 (2010) 3313–3322. doi:10.1016/j.carbon.2010.05.004.

[25] R.B. Fidel, D.A. Laird, M.L. Thompson, Evaluation of Modified Boehm Titration Methods for Use with Biochars, J. Environ. Qual. 42 (2013) 1771–1778. doi:10.2134/jeq2013.07.0285.

[26] L. Tsechansky, E.R. Graber, Methodological limitations to determining acidic groups at biochar surfaces via the Boehm titration, Carbon N. Y. 66 (2014) 730–733. doi:10.1016/j.carbon.2013.09.044.

[27] G.I. Senum, R.T. Yang, Rational approximations of the integral of the Arrhenius

721 function, J. Therm. Anal. 11 (1977) 445–447. doi:10.1007/BF01903696.

722 [28] M. Nuopponen, T. Vuorinen, S. Jämsä, P. Viitaniemi, The effects of a heat treatment
723 on the behaviour of extractives in softwood studied by FTIR spectroscopic methods,
724 Wood Sci. Technol. 37 (2003) 109–115. doi:10.1007/s00226-003-0178-4.

725 [29] E.-M.A. Ajuong, M.C. Breese, Fourier Transform Infrared characterization of Pai
726 wood (Afzelia africana Smith) extractives, Holz Als Roh- Und Werkst. 56 (1998) 139.
727 doi:10.1007/s001070050285.

728 [30] E.-M.A. Ajuong, M. Redington, Fourier transform infrared analyses of bog and modern
729 oak wood (Quercus petraea) extractives, Wood Sci. Technol. 38 (2004) 181–190.
730 doi:10.1007/s00226-004-0236-6.

731 [31] R.C. Sun, X.F. Sun, Identification and quantitation of lipophilic extractives from wheat
732 straw, Ind. Crops Prod. 14 (2001) 51–64. doi:10.1016/S0926-6690(00)00088-1.

733 [32] Y. Huang, X. Yin, C. Wu, C. Wang, J. Xie, Z. Zhou, L. Ma, H. Li, Effects of metal
734 catalysts on CO2 gasification reactivity of biomass char, Biotechnol. Adv. 27 (2009)
735 568–572. doi:10.1016/j.biotechadv.2009.04.013.

736 [33] C.Z. Li, Importance of volatile-char interactions during the pyrolysis and gasification
737 of low-rank fuels - A review, Fuel. 112 (2013) 609–623.
738 doi:10.1016/j.fuel.2013.01.031.

739 [34] D. Fuentes-Cano, F. Parrillo, G. Ruoppolo, A. Gómez-Barea, U. Arena, The influence
740 of the char internal structure and composition on heterogeneous conversion of
741 naphthalene, Fuel Process. Technol. 172 (2018) 125–132.
742 doi:https://doi.org/10.1016/j.fuproc.2017.12.015.

743 [35] M. Molina-Sabio, M.T. Gonzalez, F. Rodriguez-Reinoso, A. Sepúlveda-Escribano,

Effect of steam and carbon dioxide activation in the micropore size distribution of activated carbon, Carbon N. Y. 34 (1996) 505–509. doi:10.1016/0008-6223(96)00006-1.

[36] F. Rodríguez-Reinoso, M. Molina-Sabio, M.T. González, The use of steam and CO2 as activating agents in the preparation of activated carbons, Carbon N. Y. 33 (1995) 15–23. doi:10.1016/0008-6223(94)00100-E.

[37] E. Biagini, P. Narducci, L. Tognotti, Size and structural characterization of lignin-cellulosic fuels after the rapid devolatilization, Fuel. 87 (2008) 177–186. doi:10.1016/J.FUEL.2007.04.010.

[38] W. Zieliński, A. Rajca, Metody spektroskopowe i ich zastosowanie do identyfikacji związków organicznych: praca zbiorowa, Wydawnictwa Naukowo-Techniczne, 2000.

[39] R.M. Silverstein, F.X. Webster, D.J. Kiemle, S. Jankowski, M. Potrzebowski, M. Sochacki, Spektroskopowe metody identyfikacji związków organicznych, 2007.

[40] A. Pathak, S. Rastogi, Theoretical infrared spectra of large polycyclic aromatic hydrocarbons, Spectrochim. Acta Part A Mol. Biomol. Spectrosc. 67 (2007) 898–909. doi:https://doi.org/10.1016/j.saa.2006.09.007.

[41] E. Apaydin-Varol, A.E. Pütün, Preparation and characterization of pyrolytic chars from different biomass samples, J. Anal. Appl. Pyrolysis. 98 (2012) 29–36. doi:10.1016/j.jaap.2012.07.001.

[42] K.B. Cantrell, P.G. Hunt, M. Uchimiya, J.M. Novak, K.S. Ro, Impact of pyrolysis temperature and manure source on physicochemical characteristics of biochar, Bioresour. Technol. 107 (2012) 419–428. doi:10.1016/j.biortech.2011.11.084.

[43] Y. Chun, G. Sheng, C.T. Chiou, B. Xing, Compositions and Sorptive Properties of

767 Crop Residue-Derived Chars, Environ. Sci. Technol. 38 (2004) 4649–4655.
768 doi:10.1021/es035034w.

769 [44] W. Song, M. Guo, Quality variations of poultry litter biochar generated at different
770 pyrolysis temperatures, J. Anal. Appl. Pyrolysis. 94 (2012) 138–145.
771 doi:https://doi.org/10.1016/j.jaap.2011.11.018.

772 [45] M. Melzer, J. Blin, A. Bensakhria, J. Valette, F. Broust, Pyrolysis of extractive rich
773 agroindustrial residues, J. Anal. Appl. Pyrolysis. 104 (2013) 448–460.
774 doi:10.1016/j.jaap.2013.05.027.

775 [46] T. Dong, J. Wang, C. Miao, Y. Zheng, S. Chen, Two-step in situ biodiesel production
776 from microalgae with high free fatty acid content, Bioresour. Technol. 136 (2013) 8–
777 15. doi:https://doi.org/10.1016/j.biortech.2013.02.105.

778 [47] W.H. Schuller, C.M. Conrad, Thermal Behavior of Certain Resin Acids., J. Chem. Eng.
779 Data. 11 (1966) 89–91. doi:10.1021/je60028a024.

780 [48] J.H.P. Tyman, R.A. Johnson, M. Muir, R. Rokhgar, The extraction of natural cashew
781 nut-shell liquid from the cashew nut (Anacardium occidentale), J. Am. Oil Chem. Soc.
782 66 (1989) 553–557. doi:10.1007/BF02885447.

783 [49] A. Sarı, A. Biçer, A. Karaipekli, C. Alkan, A. Karadag, Synthesis, thermal energy
784 storage properties and thermal reliability of some fatty acid esters with glycerol as
785 novel solid–liquid phase change materials, Sol. Energy Mater. Sol. Cells. 94 (2010)
786 1711–1715. doi:https://doi.org/10.1016/j.solmat.2010.05.033.

787 [50] P. Jandura, B. Riedl, B. V Kokta, Thermal degradation behavior of cellulose fibers
788 partially esterified with some long chain organic acids, Polym. Degrad. Stab. 70 (2000)
789 387–394. doi:https://doi.org/10.1016/S0141-3910(00)00132-4.

[51] A. Ahmed, H. Pakdel, C. Roy, S. Kaliaguine, Characterization of the solid residues of vacuum pyrolysis of Populus tremuloides, J. Anal. Appl. Pyrolysis. 14 (1989) 281–294. doi:https://doi.org/10.1016/0165-2370(89)80004-X.